



HAL
open science

MOVING TOWARD GREEN AIRCRAFT: MORE ONBOARD ELECTRICITY WITH AN EFFICIENT COOLING SYSTEM

Éric Schall, Nicolas Chauchat, M. Mory

► **To cite this version:**

Éric Schall, Nicolas Chauchat, M. Mory. MOVING TOWARD GREEN AIRCRAFT: MORE ONBOARD ELECTRICITY WITH AN EFFICIENT COOLING SYSTEM. THE 28TH INTERNATIONAL CONFERENCE ON EFFICIENCY, COST, OPTIMIZATION, SIMULATION AND ENVIRONMENTAL IMPACT OF ENERGY SYSTEMS, 2015, pau, France. hal-02154253

HAL Id: hal-02154253

<https://univ-pau.hal.science/hal-02154253>

Submitted on 3 Jun 2021

HAL is a multi-disciplinary open access archive for the deposit and dissemination of scientific research documents, whether they are published or not. The documents may come from teaching and research institutions in France or abroad, or from public or private research centers.

L'archive ouverte pluridisciplinaire **HAL**, est destinée au dépôt et à la diffusion de documents scientifiques de niveau recherche, publiés ou non, émanant des établissements d'enseignement et de recherche français ou étrangers, des laboratoires publics ou privés.

MOVING TOWARD GREEN AIRCRAFT: MORE ONBOARD ELECTRICITY WITH AN EFFICIENT COOLING SYSTEM

E. Schall^a, N. Chauchat^b and M. Mory^c

^a *Corresponding author: IPRA-SIAME, UFR Sciences et techniques de Pau, Avenue de l'Université, 64013, PAU, France, eric.schall@univ-pau.fr (CA).*

^b *IPRA-SIAME, UFR Sciences et techniques de Pau, Avenue de l'Université, 64013, PAU, France, nicolas.chauchat@univ-pau.fr,*

^c *Université de Pau et des Pays de l'Adour, ENSGTI-SIAME, rue Jules Ferry, BP 7511, 64075 PAU Cedex, France. mathieu.mory@univ-pau.fr.*

Abstract:

Aircraft electrical systems are growing in all aeronautical programs. Facing increasing onboard electronic devices, more and new cooling systems have to be investigated. In this paper, particular attention is paid to the cooling of a small turbo engine represented by a heating cylinder. This new cooling industrial process designed at Pau University provides an original experimental set-up. Due to the confinement of the motion fluid flow, only experimental measurements of medium physical values like temperatures and velocity can be done. In order to better understand and with the aim of mastering such cooling system, which seems to have many industrial applications, two different numerical simulations have been investigated. Indeed, the relative low speed of the flow ($V=6.13$ m/s, $Mach=0.018$ and $Re=6500$) moving into such a complex geometrics does not enable to rule on some physical hypotheses like compressibility and stationarity. Therefore, the incompressible model is carried out using ANSYS-FLUENT software while the compressible one is conducted with *elsA* software. According to both modelling respectively with both codes, we try to identify some of the challenges that the very vast community who works on low Mach problems for many years used to meet. This study is carried out on two different scales. On the coarse scale, a good agreement between the experiment and one of the 2D simulations on the global convective wall heat flux (better than a 10% relative gap) can be observed. On the smaller scale, code-to-code comparisons of both assumptions (via both codes) show different vortex structures inside the domain. These vortices have notable but moderated influence on the inner-wall heat flux behaviours since their average values do not vary by much.

Keywords:

Air jet impact, Axis-symmetric cooling system, Comparison between compressible and incompressible flows, Green aircraft, Heating cylinder, Heat flux transfer, Low Mach number.

1. Introduction - Context

For several reasons, economic, pollution, fuel saving, environmental ... the use of more electricity seems to be unavoidable. Aerospace like other industrial sectors are not an exception to the rule. The aviation industry is committed to the revolution in energy systems on board aircraft, which will see the gradual replacement of hydraulic and pneumatic energy by electricity. For a long time, the aeronautic sector has favoured hydraulic energy, an efficient solution, which however suffers serious disadvantages. Indeed, because of aircraft movements, leaking are possible where connections between components are located. Furthermore, circuits are interdependent and if one fails, the other cannot take over. Hydraulic fluid, for its part, is corrosive and flammable. To address these risks, new source of energies must be researched. Already rather present in low power devices, electricity is now being planned for more powerful applications. Recent research work like

GREENAIR (7th RTD European framework programme) or the recent technological achievements on the A380 as on the Boeing 787 demonstrates that the use of electricity onboard is increasing.

As the use of electric-electronic devices increases, efficient cooling systems are required. The present study is part of a performance evaluation study of cooling systems for a turbo engine housing represented as a small heating cylinder. This research project has been awarded a grant coming from the DGCIS research funds (France) for four years on end after getting the aeronautics industry quality certification label from the three French aeronautical hubs. The original studied device can represent any small-sized engine and seems to have a huge potential for industrial applications. Moreover, it is not restricted to the aeronautics sector. To the best of our knowledge, there is no other research work on such cooling systems in the scientific literature.

Main objective of the paper is to improve knowledge of such cooling process. In order to achieve that, the authors proceed by experiment-numerical and numerical-numerical comparisons in two main directions. First comparison (experiment-numerical) deals with the convective heat flux transfer between the entrance fluid and the exit. This comparison is global i.e. at large scale. Then a finer study has been done through numerical-numerical comparisons for considering the effect of the compressibility. This step is unavoidable since the authors do not know about it looking at the initial conditions ($V=6.13$ m/s, $Mach=0.018$ and $Re=6500$). As numerical simulations provide physical solutions at scaled-particle, those finer comparisons are being undertaken especially on the wall heat flux behaviours. The comparison between experimental and numerical solutions is important but objective and consistent analysis of the results is not that easy even if comparison remains proper. Indeed, in view of the significant number of parameters to control, sources of errors are important and not easy to locate. In the two next paragraphs, we try to identify globally errors that come from the experiment and the numerical simulation to adjust the frame of the discussion in section 4.

From the experimental point of view:

It is worth being noticed, that the confined aspect of the set-up reduces the experimental measurement to only intrusive measures (cf section 2). Although the possibility of errors also exists, no specific study will be conducted on this matter. In this study, measurements of the temperatures and of the flow rate velocity respectively by thermocouples and flowmeter are used to fix the boundary and initial conditions for the numerical simulation. Finally, it should be noted that the temperature measurement given by the thermocouples are considered as global or on average.

From the numerical point of view:

Compared to experiment, numerical difficulties have to be taken into account differently. Assumptions must be done before calculations. At least one single reason: no modelling associated to its numerical method is able to predict any fluid flow whichever the velocity magnitude or Mach number is. It could be mentioned that the previous sentence applies to any numerical simulation with respect to a good estimate of accuracy, robustness and efficiency. The modelling through the partial difference equations (PDE) ensues from the conservative macroscopic¹ balance of the density, the momentum and the energy. While the experiment provided global physical values reduced to average temperature or medium velocity, numerical simulation can give any of the physical values (density, pressure, temperature and velocity) at the scale factor of the fluid particle.

In this paper, the main discussion concerns the compressibility. Indeed, as the chosen velocity is relatively low (6.13m/s for a Mach number worth about 0.018), taking into account or not the compressibility of the fluid is a fair question. The steady or unsteady aspect is more difficult to select because the mass flow rate is a priori constant given by the experiment. Of course, some instabilities can arise but it is hard to predict. As announced before, the sub-objective here is to make comparisons on the same simulation (i.e. with the same initial boundary conditions) between those two different assumptions. To this end, two significant softwares in their field of expertise

¹ macroscopic means on the scale factor of a fluid particle

have been chosen. Incompressible assumption will be computed with ANSYS-FLUENT while the compressible one will be computed with *elsA*.

The organization of the present work consists of four others following sections. The original set-up is described in next section "Experimental design". Once the test case is defined, the numerical strategy through a succinct presentation of the specific modelling used in the two softwares is given on section 3. Results via comparisons of both numerical-numerical and experiment-numerical are the topic of discussion in next section "Commented results". The numerical-numerical comparison is done according the two used modelling with both softwares. Finally a conclusion will summarize some of the main difficulties of such study is done in the last section. The nature of the perspectives gives some of the very big challenges expecting in numerical simulations for future.

2. Experimental design

The experimental set-up achieves the cooling of the surface of a circular cylinder (radius $R_i=5.4\text{cm}$) by 4 plane jets impacting perpendicularly the heated cylinder. As shown in Fig. 1, the four impacting jets (blue arrows) are directed from the north, east, south and west, respectively. The heated air is extracted through four outlet slots (red arrows), the directions of which are along the angle bisector between neighbouring inlet jets. The flow is confined in the annular domain with internal radius R_i and external radius $R_f=7\text{cm}$. The slot width is $S_f=3.6\text{mm}$. Numerical simulations were carried out assuming 2D flow, i.e. it does vary in the direction Oz perpendicular to the cross-section shown in Fig. 1. The cylinder length is $L=4.7\text{cm}$ in the experiment.

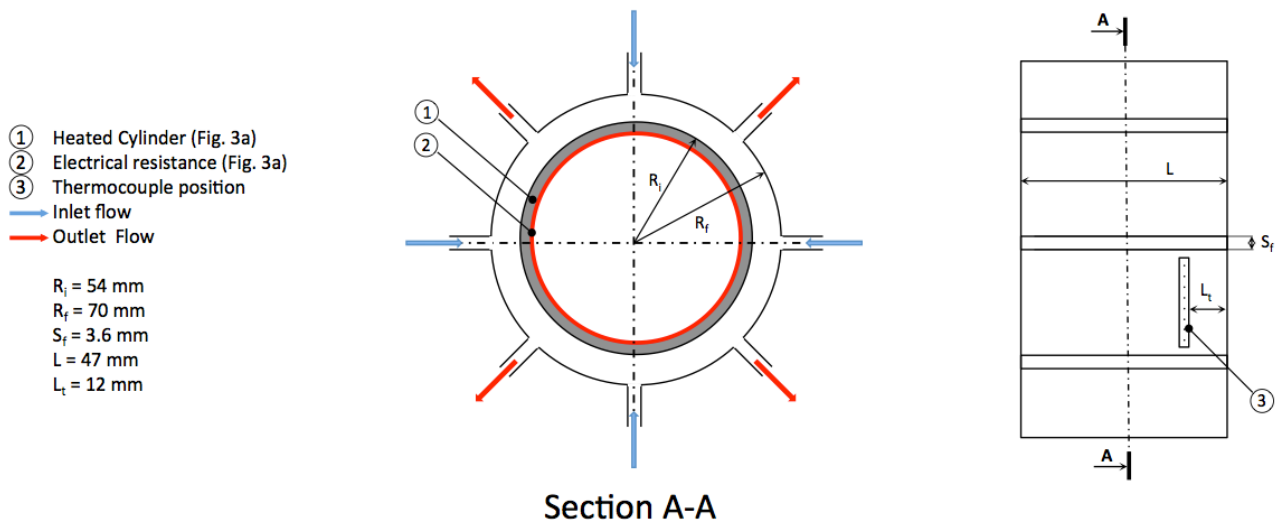


Fig. 1. View and cross-section (Section A-A) of the cooling process with the heated cylinder of radius R_i .

Photograph in Fig. 2a shows the experimental set-up. The blue arrows indicate the flow into four rectangular tubes leading to the cavity entrance slots. The casing ensuring the inlet distribution of the jets impacting the cylinder and collecting the warm air outside the flow cavity is shown in Fig. 2b. The heated cylinder is inserted under the cone seen in Fig. 2b, which channels the exit warm air into the vertical tube seen in Fig. 2a. The red arrow indicates the direction of the outlet flow into a flexible tube, which is downstream connected to a mass flowmeter (Eldridge 9700MPNH), a fan and a vane. Note that the red arrow in Fig. 2a is the convergence point of the four red arrows (seen in Fig. 1), owing to a specific air-circulation design of the heating module (seen in Fig. 2b). The circular cylinder is heated using a 250W electrical resistance inserted inside an adhesive polyamide mat glued over the inner surface of the cylinder (brown in Fig. 3a). The surface temperature on the cylinder is measured using thermocouples (type K). The thermocouples wires (green in Fig. 3a) traverse the mat and the cylinder (thickness 2mm) and the measuring extremities are bended after coming up to the cylinder surface. The entire surface of the cylinder is eventually wrapped in an adhesive film (supporting high temperature), which maintains the

thermocouples in contact with the cylinder. Fig. 3b gives an external view of the cylinder where are shown the thermocouples measurement locations.

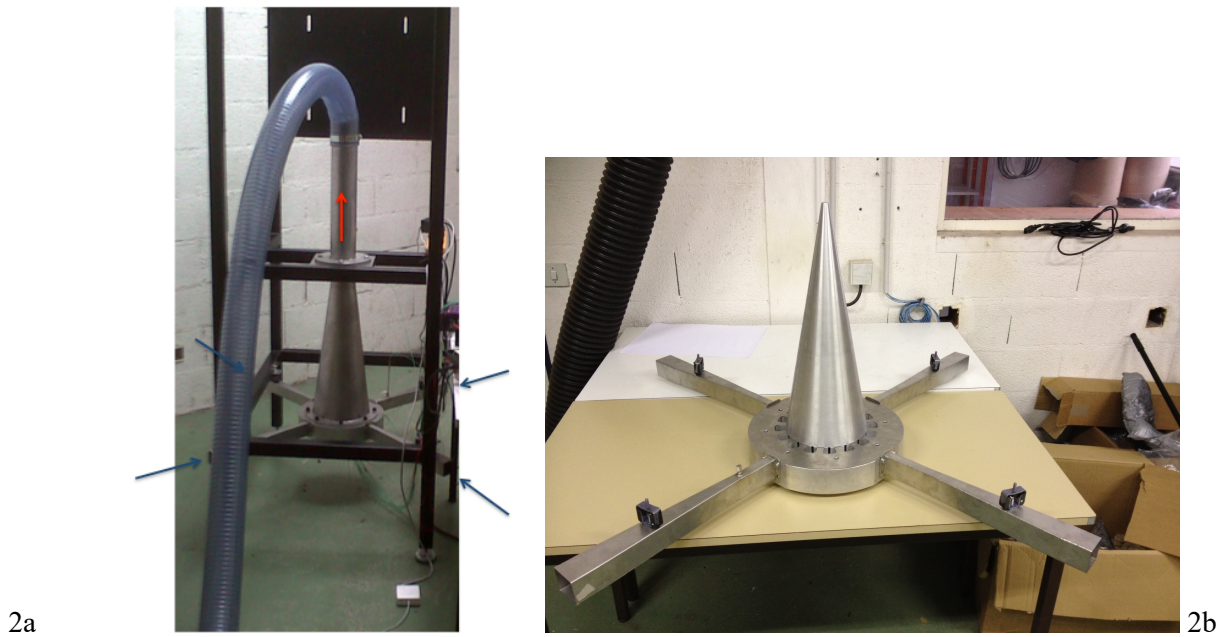


Fig. 2. Photographs of the experimental set-up. 2a The blue arrows indicate the air entrance while the red arrow represents the exit. 2b Global view of the heating module with the four branches where the air flow enters.

The schematic at the bottom indicates that thermocouples 8, 9 and 12 are along the axis line of an impacting jet, whereas thermocouples 1, 10 and 11 are along the axis line of an outlet slot.

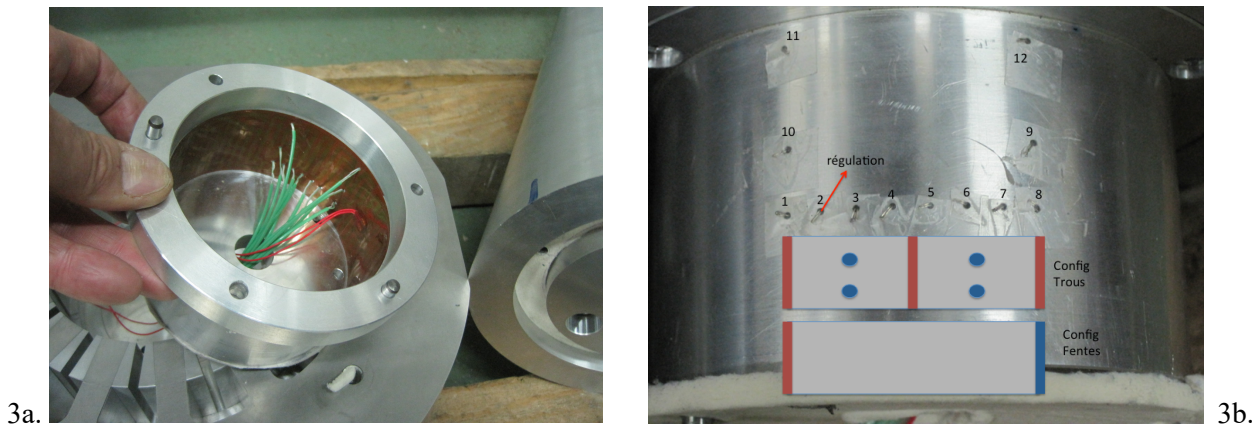


Fig. 3a. Inside view of the heated cylinder. Fig. 3b. Outside surface view of the heated cylinder showing the thermocouple positions. See Fig. 1 to locate the cylinder inside the cooling system.

The experimental conditions given by the mass flow rate and the electrical power Pelec results in the steady regime in the temperature level at the surface of the cylinder, which corresponds to the equilibrium between the furnished power and the cooling convective power. The present paper focuses on a flow condition with a relative low Reynolds number in complex geometrics. Under such conditions, the electrical power delivered was reduced as compared to the maximum electrical power (420W) in order to maintain the surface temperature less than 100°C (maximum temperature supported by the resistance polyamide mat). The electrical power delivered was measured using a wattmeter. The thermal power $\Phi_{conv} = \dot{m}c_p(T_e - T_i)$ was also estimated from the temperature difference measured by two thermocouples (type K), one being placed inside one of the inlet tube (T_i) and the

other (T_e) at the exit of an outlet slot from the cavity. An estimate of the average surface temperature T_{surf} was determined from the thermocouple measurements on the cylinder surface.

The present paper mainly deals with the ability of different numerical models to determine the heat transfer, under moderate Reynolds number conditions. We therefore more basically compare, for a selected moderate Reynolds number, the couple of values including convective thermal power Φ_{conv} and temperature difference ($T_{surf} - T_i$), obtained from different numerical simulations out of the experimental findings.

3. Numerical strategy

Numerical simulation could consist of two steps, which can be *modelling* and *numerical*. Any programmer or software user involved in computational fluid dynamics needs to be comfortable with the physical reality of the case under study. A good knowledge of the case provides the awaited partial difference equations (PDE) to compute; this is *modelling*. Then the *numerical* part deals with the numerical method to solve by computation. Difficulties with computing arise mainly from the choice of the couple (*modelling-numerical*). To begin, assumptions are done starting from the stronger to the lower ones until the computed result seems to be fair or until the *modelling* is considered as close as possible regarding the physical reality of the case.

Since the air is moving at low speed ($V=6.13$ m/s, Mach=0.018 and Re=6500) in such a complex geometrics, hypothesis on fluid compressibility is relevant but difficult to fix. Indeed, it is well known that the numerical resolution of the discrete form given by the PDE coming from the continuous model, leads to significant problems when the Mach number approaches zero ($M \rightarrow 0$), especially regarding the degree of compressibility. On one hand the community who works on incompressible flows would like to extend its application domains at least on the weakly compressible ones; however acoustic phenomena is not included in the incompressible modelling since density is constant. On the other hand, the community who deals with compressible flows would like predict low speed flows with accuracy. One knows that the original set of the compressible PDE with its numerical resolution methods which are supposed to give accurate solutions when flows are the seat of interface problems (shocks, expansion waves or rarefactions) will provide a degeneration of the pressure field. That is the reason why two different *modelling* are investigated in this paper: the incompressible modelling (IM) with ANSYS-FLUENT and the compressible one (CM) with *elsA*. Both *modelling* are the subject of many scientific communities since the beginning of the digital age. We can cite probably the two main: people from applied mathematics rather working on IM while people from applied physics prefer CM.

ANSYS-FLUENT for incompressible :

Historically the ANSYS-FLUENT software [1,2] has extensive experience in computational fluid dynamic (CFD) for a wide range of flow regimes (even for compressible flows). In the *modelling* part, the original Navier-Stokes equations for compressible flows (i.e. PDE) have been modified in order to suppress acoustic phenomenon. Among the various possibilities the most popular is density fixed or zero velocity divergence. Different combinations of PDE are possible before *numerical*. These apparent simplifications do however not mean that PDE is easy to solve from numerical standpoints. In this study the FLUENT CFX solver used for the incompressible flow application is the pressure-based one. Traditionally, the pressure updates are obtained via the resolution of an equation, which is a combination of two of the three (mass, momentum, energy) conservation equations. A Poisson equation is often employed owing to existing very efficient solvers. Whichever will be the coupling between the mass and the momentum equations in the modelling choice, segregated solvers are widely used in incompressible models. The energy equation is then solved alongside the others.

***elsA* for compressible :**

The *elsA* [3,4] software is a multi-application CFD simulation platform especially dealing with internal and external aerodynamics from the low subsonic to the high supersonic flow regime.

Concerning *modelling*, the set of PDE is coming from the original conservative Navier-Stokes equations for compressible flow without any modification. Compared to FLUENT, numerical resolution is made on the fully coupled system. It can be done with different approximate Riemman solvers based on upwind schemes. The solvers of Roe [5] and Jameson [6] have been chosen for this work.

Kind of numerical overview can be seen on Table 1 for both softwares. In particular, they are all together based on finite-volume methods under the laminar assumption. As a result, the spatial accuracy is at best of the second order. In next section, we will see that these assumptions are important in explaining some of the results.

Table 1. Numerical overview of FLUENT and *elsA*

	FLUENT	<i>elsA</i>
Version	R15.0.7	V3.3-p2
Solver	Pressured-Based	Jameson and Roe
Time	Steady	Steady
Time marching	No	Implicit – irs
Models	Energy – ON Viscous – Laminar	Navier-Stokes laminar Viscosity Sutherland
Pressure-Velocity Coupling	Scheme – Simple or Piso	
Spatial Discretisation	Gradient – Least Squares Cell Based Pressure – Standard Density – Second Order Upwind Energy – Second Order Upwind	Second order centered or upwind flux

4. Commented results

4.1. Presentation of the test case

Table 2 summarizes the physical boundary conditions for computation, which are given by the different measuring instruments (described in section 2) under standard laboratory conditions. In table 2, it must be recalled that numerical simulations are *steady* and *laminar*. Through *steady*, one understands that the physical behavior is related to an equilibrium problem. By *laminar*, it does mean that no specific *modelling* is made to capture the so-called turbulent eddies, within a wide range of length scales. Following results will emphasize the discussion about the choice of these physical assumptions.

Table 2. Physical boundary conditions.

Inlet and outlet	
Density	1.2 kg.m ⁻³
Pressure	101497.97 Pa
Inlet Temperature	294.65 K
Velocity magnitude	6.13 m.s ⁻¹
Temperature - inner/heated wall	363.15 K
Temperature - external wall	333.25 K

More technical information on the selected options of each software can be found in table 3.

Table 3. Computing conditions with FLUENT and *elsA*.

	FLUENT	<i>elsA</i>
Inlet	Massflow_inlet ² Normal of inlets ⁴ =(0, -1, 0) or (-1, 0, 0) mass flux=7.36 kg.m ⁻² .s ⁻¹ pressure = 101497.97 Pa temperature = 294.65 K	Injmfri ³ Normal of inlets ⁴ =(0, -1, 0) or (-1, 0, 0) Surface mass flow=7.36 kg.m ⁻² .s ⁻¹ Stagnation enthalpy=296054.53 m ² .s ⁻²
Outlet	Pressure_outlet ² pressure = 101497.97 Pa temperature = 294.65 K	Outpres ³ pressure = 101497.97 Pa
Internal wall (heated wall)	wall ² temperature = 363.15 K wall ²	wallisoth ³ temperature = 363.15 K wallisoth ³
External wall	temperature = 333.25 K	temperature = 333.25 K

Thanks to the geometry of the test case, we have decided to make 2D computations only on one quarter of the full cavity seen in figure 1. Then, axial symmetric conditions are supposed where $x=0$ and $y=0$. $y=0$ and $x=0$ are the basic axes oriented respectively horizontally and vertically. However, while motivated by computational time-saving, this geometrical choice will lead some disadvantages as mentioned below. Details on grids are given in table 4. Even though grid cells are different between both softwares, the minimum size of the edge belonging to the inner-heated wall is of the same order of magnitude for the sake of accuracy. Concerning the lines 4 and 5 of table 4, the parietal grid repartition is constant for FLUENT and is geometric for *elsA*. This is the reason why a couple of number stays in the *elsA* column. Last but not the least, final computations were carried out after systematic studies of grid convergence with both codes. Undoubtedly, readers may be surprised when considering the difference of the cell numbers used by the two codes. For saving time and practical reasons, concerning *elsA* computations, we have decided to build the domain without the slots.

Table 4. Grid breakdown for FLUENT and *elsA*.

	FLUENT	<i>elsA</i>
Number of points	111 739	11 908
Number of cells	246 609	11 628
Cell geometry	Triangular	Quadrangular
Min and max edge size on the inner-heated cylinder (m)	$1.3e^{-5}$	$6.2e^{-5}$ to $1.1e^{-3}$
Min and max edge size on the outer cylinder (m)	$5.1e^{-4}$	$8.1e^{-5}$ to $1.4e^{-3}$

4.2. ANSYS-FLUENT computations

First of all, under the assumption of incompressible flows, two computational simulations are made with two discretisation schemes, which are SIMPLE [7] and PISO [8]. These numerical algorithms are of the pressure-based family.

In both computations usual convergence criteria available in FLUENT are not satisfied after 300000 iterations. A transitional phase is observed for the first 20000 iterations. Then a flow regime more or less stable takes place in the central part of the cavity outside the viscous boundary layers. These instabilities can be seen in figures 4a and 4b through the eddy patterns represented by streamlines. Nevertheless when compared to SIMPLE the solution obtained with the PISO algorithm is more stable.

² See Fluent user's guide

³ See the User's reference manual of *elsA*

⁴ In the flow direction

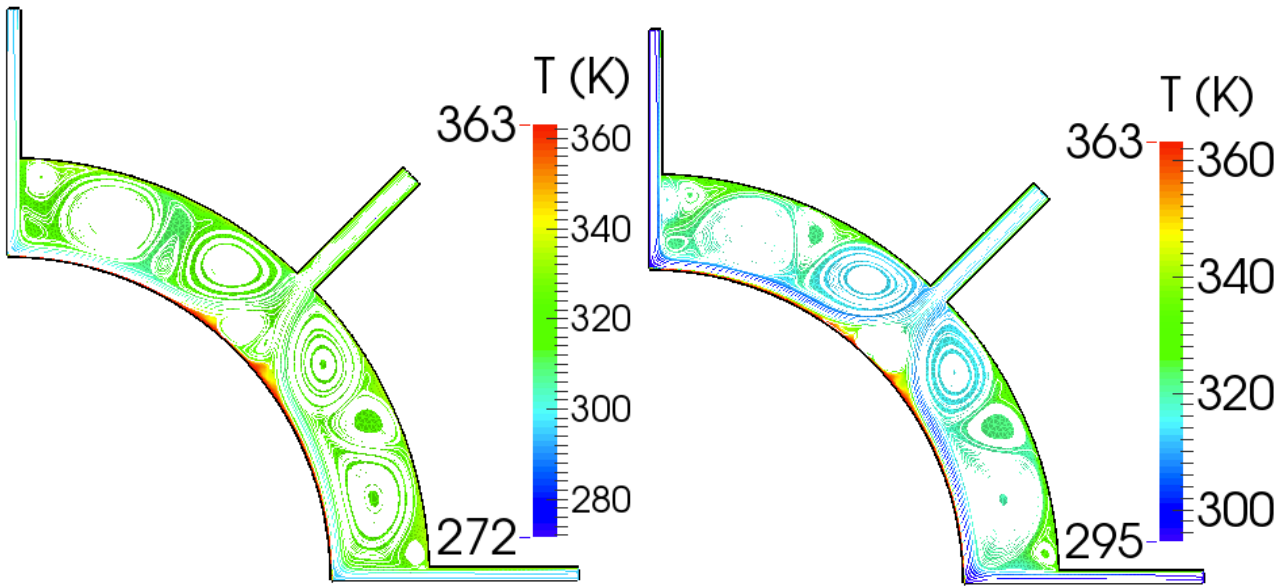


Fig. 4a. Left: Streamline and temperature in a quarter domain with FLUENT+SIMPLE.

Fig. 4b. Right: Streamline and temperature in a quarter domain with FLUENT+PISO.

Figure 5 (like figure 8) represents the evolution of the conductive wall heat flux at the inner wall. This flux is the consequence of the 250W electrical resistance inserted on the inner surface of the cylinder (remember figure 3a). Because of power leaks, conductive heat flux is deduced from a wall temperature obtained by an average out of the 10 parietal thermocouples (see section 2).

Despite the complexity and motion of the eddy patterns, the conductive heat flux evolution remains the same, as seen in figure 5. The amount of the energy absorbed by the moving eddies is relatively apparently weak.

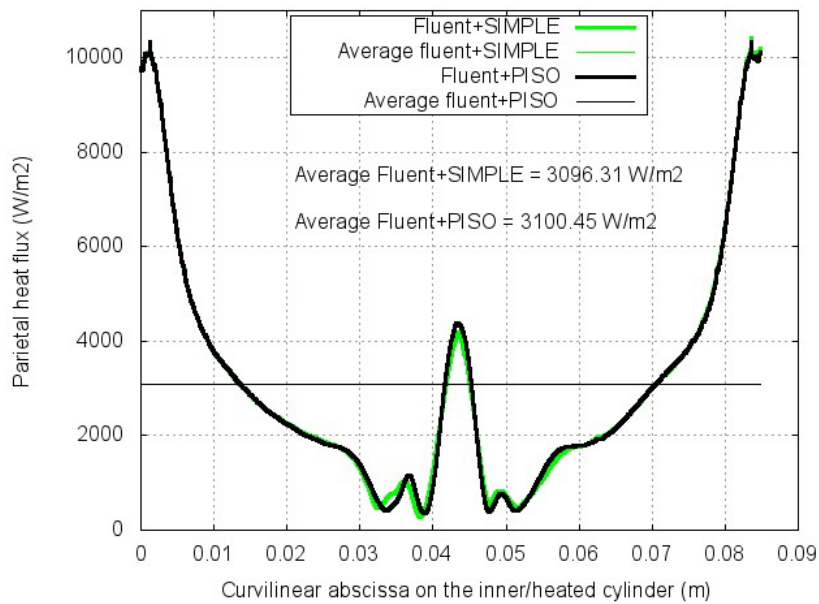


Fig. 5. Parietal evolution of the conductive heat flux of the inner-heated cylinder with FLUENT.

4.3. elsA computations

In a second step, under the assumption of compressible flows, two computational simulations are done with two different approximate Riemann solvers, which are commonly known as Jameson and Roe.

The steady state is reached after 300 000 time iterations as seen on figure 6 for both solvers even if their evolutions are different. Residual on the density (like any other physical conservative variables) has lost at least 10 orders of magnitude on both calculations, and solutions are stable.

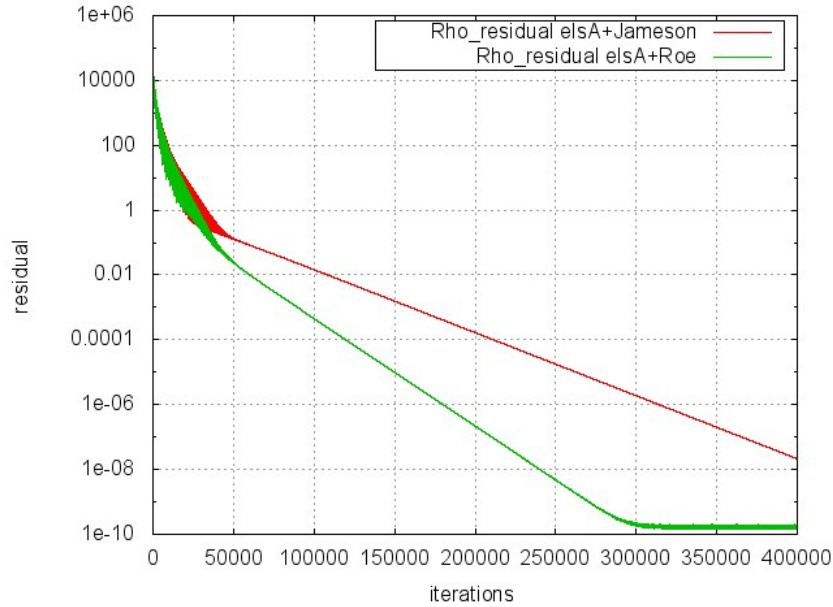


Fig. 6. Convergence history on the density (Rho).

Figures 7a) and 7b) confirm previous findings on the stability. The eddy patterns are reduced to four distinctive vortices in a perfect symmetry.

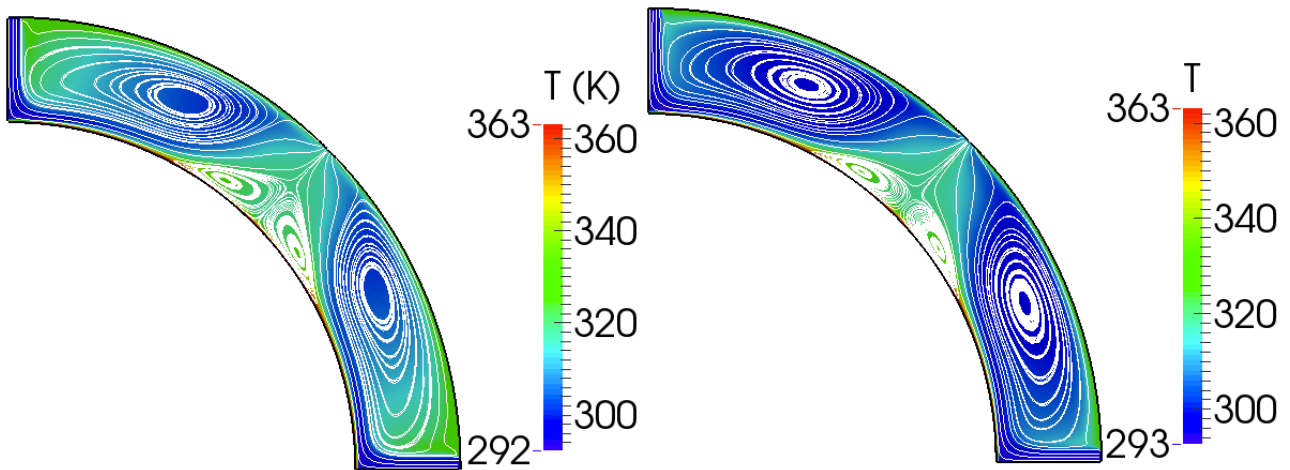


Fig. 7a. Left: Streamline and temperature in the carter with *elsA*+Jameson.

Fig. 7b. Right: Streamline and temperature in the carter with *elsA*+Roe.

In figure 8, heat flux behaviours of both solutions are mainly the same excepted where the air jets impact ($x=0m$ and $x=0.084m$) and where the flow exists ($x=0.042m$). Averages on both fluxes are equivalent at less than 4.5% in relative value.

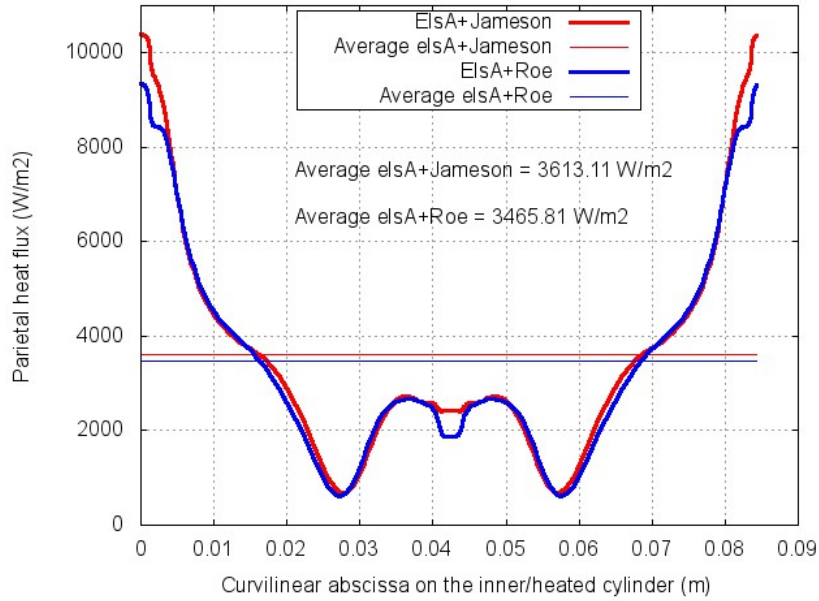


Fig. 8. Parietal evolution of the conductive heat flux of the inner-heated cylinder with *elsA*.

4.4. Comparisons FLUENT- *elsA* and Numerical-Experiment

Percentages of error on mass flow rate are given in table 5 for the 4 computations. For each case, the inlet mass flow rate is the reference. With FLUENT, errors are in a range between 2% and 7.3% with PISO and SIMPLE. Although the SIMPLE solution is the most volatile the estimation on the exit mass flow rate is better than of PISO. With *elsA*, errors are lower by three orders of magnitude (in absolute value) compared to those obtained with FLUENT. This difference in accuracy can originate from the mesh size which varies between FLUENT and *elsA* computations. As well, the missing slots of the *elsA* computational domain can explain such a difference. In any case for future work, that point should deserve special attention.

Table 5. Error on the inlet/outlet mass flow rate with FLUENT and *elsA*.

	Experiment	FLUENT with SIMPLE	FLUENT with PISO	<i>elsA</i> with Jameson	<i>elsA</i> with Roe
Inlet mass flow rate (kg.s ⁻¹)	0.001245	0.001176	0.001176	0.001241	0.001239
Error rate (over the experiment)		-5.5%	-5.5%	-0.3%	-0.5%
Outlet mass flow rate (kg.s ⁻¹)	0.001245	0.001199 to 0.001242	0.001208 to 0.001262	0.001243	0.001243
Error rate of the outlet mass flow over inlet		2.0% to 5.6%	2.7% to 7.3%	0.001%	0.003%

In Table 6 convective heat fluxes are given, respectively with FLUENT and *elsA*. Comparisons are given between computations and experiment. The volatility of the SIMPLE algorithm is demonstrated with an error rate of between -53% and -7%. Concerning PISO, the error rate is hovering around the experimental result in a range between -11% and 8%, which confirms a more stable solution compared to that of SIMPLE as announced before.

Table 6. Convected heat flux comparisons with FLUENT and *elsA*. Experiment is the reference.

	Experiment	FLUENT with <i>SIMPLE</i>	FLUENT with <i>PISO</i>	<i>elsA</i> with Jameson	<i>elsA</i> with Roe
Convected heat flux (W)	27.65	13.03 to 25.80	24.43 to 29.88	25.23	21.39
Error rate (over the experiment)		-53% to -7%	-11% to 8%	-8%	-22%

Though *elsA* solutions are stable, the error rates difference is relatively important between both solvers. Compared to the experiment the error rate is of -22% with Roe and of -8% with Jameson. Thus, a downward trend of the Roe solver compared with that of Jameson appears to be borne out.

Figure 11 depicts final comparison of the inner heat wall flux evolution between FLUENT-PISO and *elsA*-Jameson. The behaviour of these curves appears to be a consequence of the swirling structure seen in figures 4 and 7. Positions $x=0$ and $x=0.084$ correspond to the axes of two impacting jets and the respective heat fluxes are maximal as expected. Starting from these extremities both fluxes globally decrease along the cylinder before increasing in the vicinity of the outlet slot axis. Although curve profiles are not strictly identical the average values of the fluxes are the same within 16%.

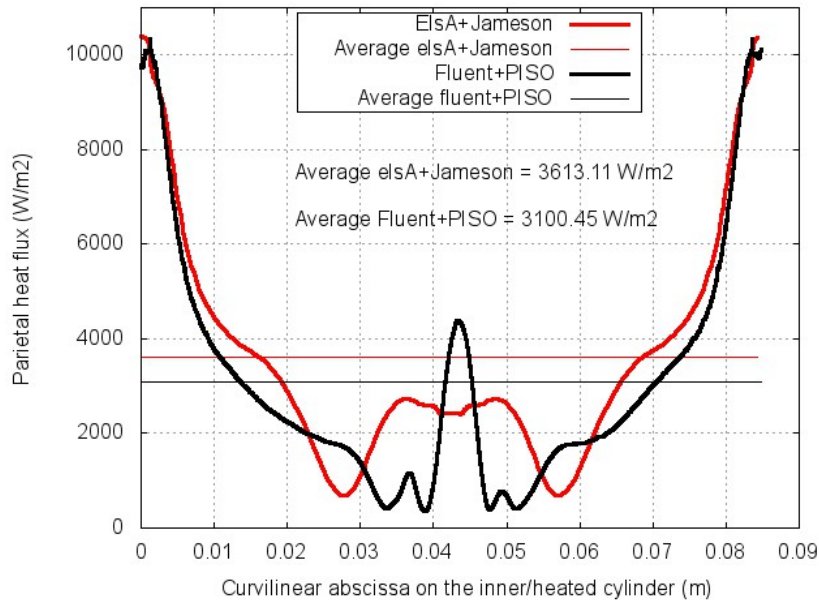


Fig. 11. Parietal inner conductive heat flux comparison between *elsA* and FLUENT.

5. Conclusion and perspectives

In the context of onboard green aircraft projects, the increasing use of electrical engines require more efficient cooling systems. In this study, a specific cooling system based on four air jet impacting on a heater cylinder has been tested. This laboratory facility, installed at Pau University (France) is devoted to the study of small-sized turbo engines.

Numerical simulations of convective heat transfer are conducted in parallel. Simulating the laboratory test case allows a comparison with experimental data, but the aim was also to achieve a comparison between numerical codes by solving the Navier-Stokes equations for incompressible or compressible fluids. This comparison is made by using the incompressible model of FLUENT and the compressible one of *elsA*.

The flow fields obtained by the two codes show eddy patterns in the simulated annular domain, which differ in detail and display unsteadiness even under steady boundary conditions. As a

consequence, the parietal inner conductive heat fluxes differ along the wall while their average values are the same within 16% (even 10% compared to the Roe solution).

The total convective heat transfer predicted by numerical simulations is in coarser agreement with the results of the laboratory experiment for the FLUENT incompressible code (ranging from 0.47 to 1.08 of the laboratory value) as compared to the results of the compressible *elsA* code (ranging from 0.77 to 0.91 of the experimental value). On the other hand the conservation of mass flow rates between inlet and outlet is better achieved by *elsA* the compressible code than by FLUENT the incompressible code. However, it is far too early to draw here any qualitative conclusion about the resulting findings in both modelling and further improvements are rather necessary.

It is encouraging that the results of simulations are in qualitative agreement with the laboratory experiments and recover the order of magnitude of the total heat transfer measured. Nevertheless, much remains to be done like 3D computations. Modelling compressible fluid flows is known to be difficult for low Mach number conditions. Our goal is orient ourselves into the development of “All Mach” solvers.

Acknowledgments

The authors would like first to thanks the Pau University (UPPA), the Conseil Régional d'Aquitaine and SAFRAN-Turbomeca for their financial support of the PhD thesis of Nicolas CHAUCHAT. Second, many thanks to ONERA for their invaluable and daily help in the best use as possible of the *elsA* software. Finally, as mentioned above, in the case of the selected research program by the three French aeronautical poles of competitiveness (Aerospace Valley, ASTech and PEGASE), part of this research was supported by Public Finance of the DGE (Direction Générale des Entreprises).

References

- [1] Franklyn J. Kelecy. Coupling momentum and continuity increases CFD robustness, ANSYS advantage, volume II, issue 2, 2008.
- [2] ANSYS Fluent software contains the broad physical modelling capabilities needed to model flow, turbulence, heat transfer, and reactions for industrial applications. Available at: <<http://www.ansys.com/Products/Simulation+Technology/Fluid+Dynamics/Fluid+Dynamics+Products/ANSYS+Fluent>> [accessed 21.1.2015].
- [3] Laurent Cambier, Sébastien Heib, and Sylvie Plot. The ONERA *elsA* CFD software : input from research and feedback from industry. *Mechanics & Industry*, 14(03) :159–174, 2013.
- [4] *elsA* is the ONERA software for complex external and internal flow simulations and for multi-disciplinary application involving aerodynamics. Available at: <<http://elsa.onera.fr>> [accessed 21.1.2015].
- [5] P. L. Roe. Approximate Riemann Solvers, Parameter Vectors, and Difference $\left[\begin{smallmatrix} L \\ SEP \end{smallmatrix} \right]$ Schemes. *J. Comput. Phys.*, 43:357–372, 1981.
- [6] A. Jameson, W. Schmidt, and E. Turkel. Numerical Solution of the Euler Equations by Finite Volume Methods using Runge–Kutta Stepping Schemes. Technical Report 81–1259, AIAA, 1981.
- [7] S.V. Patankar and D.B. Spalding, “A calculation procedure for heat, mass and momentum transfer in three-dimensional parabolic flows”, *International Journal of Heat and Mass Transfer*, Vol. 15, pp. 1787-1806 (1971).
- [8] Issa, R. I. (1986). Solution of the implicitly discretised fluid flow equations by operator-splitting, *J. Comput. Phys.*, Vol. 62, pp. 40-65.